Earth Planets Space, **61**, 913–917, 2009

The seasonal and solar cycle variations of electron density gradient scale length during magnetically disturbed days: implications for Spread *F*

G. Manju, C. V. Devasia, and Sudha Ravindran

Space Physics Laboratory, Vikram Sarabhai Space Centre, Trivandrum, 695 022 Kerala, India

(Received September 12, 2007; Revised November 28, 2008; Accepted January 9, 2009; Online published August 31, 2009)

The behaviour of electron density gradient scale length, L, around post-sunset hours during the magnetically disturbed days of the summer, winter and equinox seasons of solar maximum (2002) and minimum years (1995) has been studied, using ionosonde data of Trivandrum (8.5°N, 76.5°E, dip = 0.5°N) in the Indian longitude sector. The results indicate a clear seasonal and solar cycle variation in L. Seasonal variations of the maximum vertical drift of the F layer were also examined on these days. In particular, the seasonal variation of the Equatorial Spread F (ESF) during this period is examined in terms of the relative roles of L and the vertical drift of the F layer in the triggering of the collisional Rayleigh-Taylor instability. Our results on the clear-cut seasonal and solar cycle variation in L for disturbed days and its control of ESF occurrence are presented and discussed.
Key words: Equatorial ionosphere, ionospheric irregularities, plasma instability, Equatorial Spread F.

1. Introduction

Equatorial Spread F (ESF) is a spectacular phenomenon in which the equatorial region ionosphere is transformed after sunset. The plasma instabilities responsible for ESF occur on time scales ranging from seconds to hours and on length scales of centimetres to several hundred kilometres (Farley *et al*., 1970; Woodman and LaHoz, 1976; Fejer and Kelly, 1980; Abdu *et al*., 1981; Fejer *et al*., 1999; Hysell and Burcham, 2002). The occurrence of ESF depends on the season, solar cycle, geomagnetic activity and longitude, and it also has a highly complex day-to-day variability (Chandra and Rastogi, 1970; Abdu *et al*., 1981; Kelley and McClure, 1981; Tsunoda, 1985; Huang *et al*., 1987; Sridharan *et al*., 1994; Subbarao and Krishna Murthy, 1994; Abdu, 2001; Devasia *et al*., 2002; Jyoti *et al*., 2004; Lee *et al*., 2005). The plasma irregularities that occur in the F region also influence satellite-based communication navigation systems, leading to economic losses. Extensive experimental and theoretical research has been carried out on ESF during the last four decades to study equatorial Spread F, with the results showing that plasma instabilities play a major role in the generation of these irregularities. The primary process responsible for the generation of the irregularities is the Collisional Raleigh-Taylor (CRT) instability mechanism, which operates in the post-sunset bottom side F region (Haerendel, 1973; Costa and Kelley, 1978) under certain favourable conditions, including the movement of the F-layer to very high altitudes in the post-sunset hours and/or formation of the steep bottom side F-layer electron density gradient. The effects of meridional winds, which move plasma along field lines both vertically and horizontally, on ESF occurrence, have been examined by some researchers (Maruyama and Matuura, 1984; Maruyama, 1988). Studies on the role of seed perturbations in the generation of F region irregularities have been reported by Whitehead (1971) and Fejer *et al*. (1999).

In the study reported here, we have examined the seasonal variations of electron density scale length, L, and the vertical drift ($dh'F/dt$) of the F layer on magnetically disturbed days of solar minimum (1995–1996) and maximum (2002–2003) years. The expression for L is given by

$$L = \left(\frac{1}{n}\frac{dn}{dh}\right)^{-1} \tag{1}$$

where, n is the electron density, h is the height and (dn/dh) is the electron density gradient.

The modulation of the seasonal pattern of post-sunset ESF occurrence (during magnetically disturbed days) by the seasonal variations of L and $[d(h'F)/dt]_{\max}$ are presented and discussed.

2. Experimental Set-up and Data and Method of Analysis

Ionosonde data of Trivandrum (8.5°N, 76.5°E, dip latitude 0.5°N) in the Indian longitude sector was used in this study. The available ionosonde data for the summer, winter and autumnal equinox seasons of 1995–1996 (solar minimum) and 2002–2003 (solar maximum) were examined. The reader should note that the term "equinox" in subsequent discussions and in all figures refers to the autumn equinox (September–October).

The phenomenon of ESF is the result of a hierarchy of multistep, nonlocal plasma processes involving the collisional and collision-less Rayleigh-Taylor (R-T) and $\mathbf{E}\times\mathbf{B}$

instabilities as well as drift waves driven by coupled electrodynamic and neutral atmospheric processes (Haerendel, 1973; Zalesak *et al.*, 1982; Sekar and Kelley, 1998). We examined the role of the CRT instability mechanism in producing the observed seasonal occurrence pattern of ESF on magnetically disturbed days.

The expression for the growth rate of the generalized R-T instability in terms of different forcing parameters is given as (Sekar and Raghavarao, 1987)

$$\gamma = \frac{1}{L}\left(\frac{g}{\nu_{\text{in}}} + \frac{E_x}{B} + W_x\frac{\nu_{\text{in}}}{\Omega_i} - W_z\right) \qquad (2)$$

where E_x is the zonal electric field, B is the geomagnetic field, g is the acceleration due to gravity, ν_{in} is the ion-neutral collision frequency, Ω_i is the gyrofrequency, and W_x and W_z are the zonal and vertical winds, respectively.

The role of winds and seed perturbations modulates the day-to-day occurrence pattern of ESF, even on days when the first term in Eq. (2) is unfavourable. Our aim was to examine the degree to which the CRT mechanism accounts for the general seasonal pattern of ESF when only variabilities in L and ν_{in} are considered. We have therefore considered only ESF events occurring up to or preceding 2100 hours.

The L and $d(h'F)/dt$ values in the post-sunset period of each day are deduced. While there are no direct measurements of ν_{in}, it is known that ν_{in} decreases with height and that an increased upward (downward) vertical drift necessarily indicates the movement of the layer into a region of lower (higher) ν_{in}. Consequently, for this study, an upward vertical drift is taken to correspond with a decrease in ν_{in}, and vice versa. Whether the layer height on its own can also modulate the ESF occurrence pattern was beyond the scope of our study.

As mentioned, L is given by, $L = [(1/n)(dn/dh)]^{-1}$, where dn/dh is obtained by considering the virtual heights of reflection at 2 MHz and 3 MHz, respectively.

The scaling accuracy of $h'F$ is 3 km. The error in dn/dh obtained by using $h'F$ instead of the true height is estimated to be less than 5% (Krishna Murthy *et al.*, 1990). This error is low because the difference between the virtual and true heights is rather small at these low frequencies, during the night time, due to negligible underlying ionisation. The vertical drift of the F layer is obtained by deducing $d(h'F)/dt$. Here, the vertical drift due to recombination effects is neglected as it is not significant in relation to the large vertical drift due to the pre-reversal enhancement of the zonal electric field (Tulasi Ram *et al.*, 2006). The L and maximum $d(h'F)/dt$ values are estimated for available data on each day, corresponding to the three seasons of solar minimum (1995–1996) and solar maximum (2002–2003). The maximum vertical drift in the post-sunset hours and the L value on each day are used to interpret the seasonal pattern of ESF.

3. Results

In this study, the days with $A_{\text{p}} < 18$ are considered to be magnetically quiet days and those with A_{p} value ≥ 18 are considered as magnetically disturbed days.

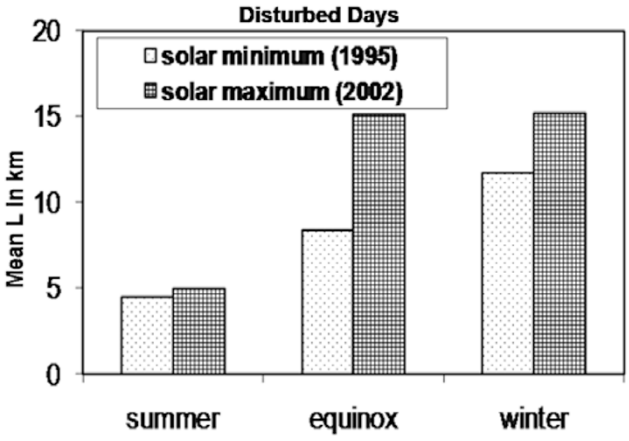

Fig. 1. Seasonal variation in mean L for magnetically disturbed days of the solar minimum and maximum.

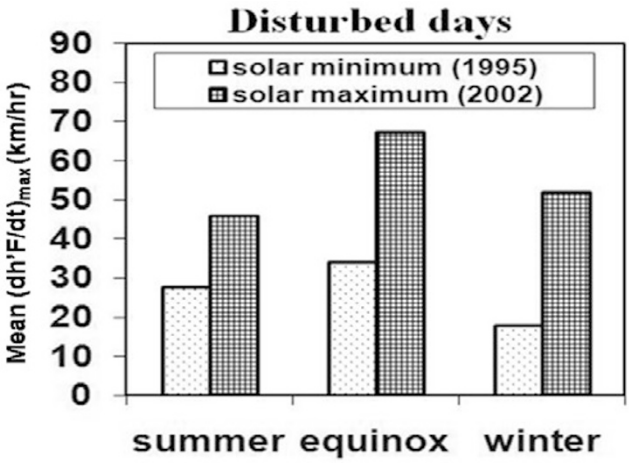

Fig. 2. Seasonal variation in mean vertical drift ($d(h'F)/dt$) for magnetically disturbed days of the solar minimum and maximum.

3.1 Seasonal variation of *L* on magnetically disturbed days

Figure 1 shows the seasonal variation of mean L for the magnetically disturbed days of solar minimum and maximum epochs. For both epochs, the mean L value is maximum during the winter and minimum during the summer. During the solar minimum, the mean L value increases from 4.5 km in the summer to 8.4 km and 11.7 km in the equinox and winter, respectively. In the solar maximum, the mean L value increases from 5 km in summer to approximately 15.2 km in the equinox/winter.

3.2 Seasonal variation of *d(h′F)/dt* on magnetically disturbed days versus quiet days

The seasonal mean of the maximum vertical drift (obtained by averaging the vertical drift on the individual days of each season) in the post-sunset hours for the magnetically disturbed period of the above three seasons of solar minimum and maximum epochs are shown in Fig. 2. The seasonal mean vertical drift velocity is at a maximum in the equinox for both solar epochs, while it is at a minimum in the winter of the solar minimum and in the summer of the solar maximum. In the solar minimum, the vertical drift increases by nearly 1.5-fold from the winter to the summer

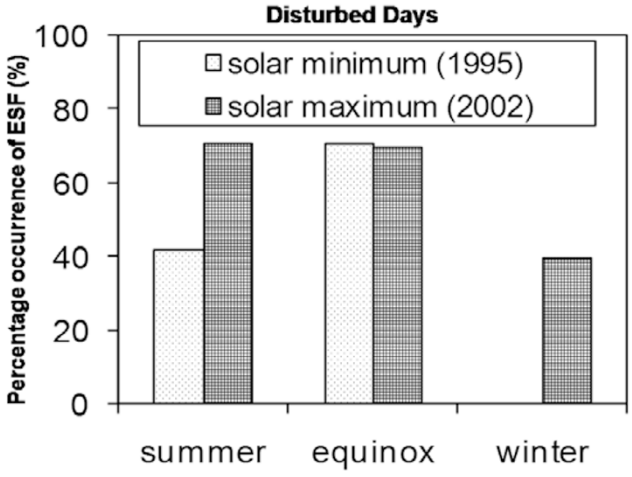

Fig. 3. Seasonal variation in percentage occurrence of ESF for magnetically disturbed days of the solar minimum and maximum.

and by nearly twofold from the winter to the equinox, while in solar maximum it increases by approximately 1.3-fold (from the winter to the equinox) and decreases by nearly 12% from the winter to the summer. Thus, the vertical drift is most favourable for the occurrence of the ESF during the equinox in both epochs.

3.3 Seasonal pattern of ESF occurrence during magnetically disturbed days of solar minimum and maximum epochs

The seasonal mean percentage occurrence of ESF during magnetically disturbed days of the solar minimum and maximum are shown in Fig. 3. During the solar minimum, there is maximum percentage ESF occurrence in the equinox and minimum occurrence in the winter; in contrast, during the solar maximum, maximum ESF percentage occurs during the summer/equinox and minimum occurrence during the winter.

4. Discussion

Here we discuss the seasonal mean percentage occurrence of ESF in association with the seasonal mean behaviour of the electron density gradient scale length L and $[dh'F/dt]_{\max}$ in order to gain an understanding of whether collisional R-T instability on its own provides an adequate explanation of the general pattern of ESF occurrence in a given season and solar epoch.

The collisional R-T instability mechanism regulates the initial growth of the ESF irregularities. For this instability to be triggered, the altitude of the bottom side F region has to be high enough and seed perturbations have to be present. Earlier studies examined the seasonal pattern of occurrence of ESF (Subbarao and Krishna Murthy, 1994), but the implications of the seasonal variations of L were not considered.

The growth rate of the collisional R-T instability is inversely related to L and ν_{in}, as seen from the first term in Eq. (2). We have examined the general occurrence pattern of post-sunset ESF in terms of variations in these two parameters. More specifically, we have looked at the mean seasonal and solar cycle dependence of L in conjunction with the corresponding variation in $d(h'F)/dt$ during the post-sunset hours. As mentioned earlier, the layer height, which can also independently modulate the ESF occurrence pattern, was not examined in this study.

For the equinox season, the mean L value increases by a factor of approximately 1.8 in during the solar maximum (with respect to solar minimum), which means it is much less favourable for ESF. Correspondingly, the mean $[dh'F/dt]_{\max}$ value increases by approximately twofold (from the solar minimum to maximum). Although the vertical drift is more favourable for ESF during the solar maximum, the L parameter tends to inhibit it. Moreover, during periods of high solar activity, the scale height (H) of the neutrals in the F region changes significantly due to increasing temperature ($H = RT/Mg$), where R is the gas constant, T is the temperature in °K, M is the molecular mass and g the acceleration due to gravity. The increase in H with increasing solar activity results in an expansion of the thermospheric neutral densities (Fuller-Rowell *et al.*, 1996) and, consequently, increasing ion-neutral collision frequencies. This in turn results in a reduced growth rate of the R-T instability (Eq. (2)) for a given altitude at solar maximum in comparison to that at solar minimum (Manju *et al.*, 2007). All these aspects act together such that a comparable percentage occurrence is seen in the equinox of both the solar minimum and maximum.

For the summer season, we observed that the mean L value increased by 1.1-fold during the solar maximum compared to the solar minimum. At the same time, the vertical drift increases by a factor of approximately 1.7. The favourable larger value of vertical drift during the summer of the solar maximum results in an increased percentage occurrence of ESF compared to the solar minimum period. The above-mentioned temperature-related effect on ion-neutral collision frequencies is also seen during the summer, but that seems not to be significant enough to affect the seasonal ESF occurrence pattern.

For the winter season, the mean L value increases by approximately 1.3-fold from the solar minimum to the solar maximum, which means that it is less favourable for the occurrence of ESF in the solar maximum. Correspondingly, the mean $[dh'F/dt]_{\max}$ value increases by more than 2.9-fold. Again, in this case the vertical drift is more favourable for ESF in solar maximum, but the L parameter is less favourable. Due to the increase in vertical drift being more significant than that in L as well as the fact that the height of the F layer itself is much higher, approximately 300 km in the winter of the solar maximum (Subbarao and Krishna Murthy, 1994), a higher percentage occurrence of ESF is observed in the winter of the solar maximum (the above-mentioned temperature-related effect on ion-neutral collision frequencies is less in winter) (Manju *et al.*, 2007).

The seasonal pattern of L and vertical drift in a given epoch was analysed to interpret the observed seasonal ESF occurrence pattern. During the solar minimum, the L value increases by approximately 1.9-fold from the summer to the equinox while the vertical drift increases by 1.2-fold. The fact that the L factor is relatively lower than in equinox favours ESF occurrence in the summer, while the vertical drift (being lesser than in the equinox, thereby keeping the

layer at a lower altitude where ν_{in} is less favourable) inhibits it. During equinox the vertical drift factor is favourable for ESF, while the L factor inhibits ESF. The higher occurrence of ESF in the equinox of the solar minimum in relation to summer indicates that the unfavourable effect of increased L in the equinox is offset by the favourable effect of the vertical drift on the growth rate of the collisional R-T instability.

The mean L value increases by approximately 2.6-fold from the summer to the winter in the solar minimum, while the mean $[dh'F/dt]_{max}$ value correspondingly decreases by a factor of 0.6., i.e. both the L and mean $[dh'F/dt]_{max}$ are very much unfavourable for the R-T instability growth rate during winter. Thus no ESF events are observed during the winter of solar minimum period.

In the case of solar maximum, the mean L value increases from the summer to the equinox by around 3.0-fold, while the mean $[dh'F/dt]_{max}$ value increases by approximately 1.5-fold. The combined effect of the two parameters would favour a higher percentage occurrence of ESF in the summer. However, it is likely that the higher layer height in the equinox season (Subbarao and Krishna Murthy, 1994) results in the ν_{in} factor being favourable so that a comparable percentage occurrence of ESF is observed in the summer and equinox seasons of the solar maximum.

The mean L value increases by around threefold from the summer to the winter in the solar maximum, with the mean $[dh'F/dt]_{max}$ value correspondingly increasing by a factor of 1.1. Here, the L factor significantly modulates (reduces) the growth rate and offsets the favourable effect of increased vertical drift in winter. This results in a lower percentage occurrence of ESF in the winter of the solar maximum compared to the summer.

In this study, we did not consider some of the factors controlling the generalized R-T instability, namely the role of the seed perturbations and winds. Our reasoning was that our aim was to gain an understanding of the degree to which the L and ν_{in} (as can be inferred from $[dh'F/dt]_{max}$) variability suffices explain the mean seasonal pattern of ESF on magnetically disturbed days. For the equinox season, the vertical drift seems to be determining the percentage occurrence of ESF. However, for the summer and winter, especially in the solar maximum, the role of L seems to substantially modulate the percentage occurrence pattern.

5. Main Results and Conclusions

The important conclusions of this study are:

i. Clear-cut seasonal variation is seen in L for the magnetically disturbed days of both the solar minimum and maximum. The L value at a minimum for the summer and at a maximum for the winter in both the solar epochs.

ii. During the magnetically disturbed period of the solar minimum, the percentage occurrence of ESF is at a maximum in the equinox and at a minimum in the winter. For the magnetically disturbed period of the solar maximum, the percentage occurrence of ESF is comparable in the summer/equinox and at a minimum in the winter.

iii. The clear-cut seasonal and solar cycle variation of L and its control on the occurrence of ESF during magnetically disturbed periods is clarified in this study.

Acknowledgments. The authors would like to thank the referees, for their valuable suggestions, which helped greatly in improving the manuscript.

References

Abdu, M. A., I. S. Batista, and J. A. Bittencourt, Some characteristics of Spread *F* at the magnetic equatorial station Fortaleza, *J. Geophys. Res.*, **86**(A8), 6836–6842, 1981.

Abdu, M. A., Outstanding problems in equatorial ionosphere-thermosphere electrodynamics relevant to Spread *F*, *J. Atmos. Sol.-Terr. Phys.*, **63**, 869–884, 2001.

Chandra, H. and R. G. Rastogi, Solar cycle and seasonal variation of Spread *F* near the magnetic equator, *J. Atmos. Sol.-Terr. Phys.*, **32**, 439–444, 1970.

Costa, E. and M. C. Kelley, On the role of steepened structures and drift waves in equatorial Spread *F*, *J. Geophys. Res.*, **83**, 4359–4364, 1978.

Devasia, C. V., N. Jyoti, K. S. Viswanathan, K. S. V. Subbarao, D. Tiwari, and R. Sridharan, On the plausible linkage of thermospheric meridional winds with equatorial Spread *F*, *J. Atmos. Sol.-Terr. Phys.*, **64**, 1–12, 2002.

Farley, D. T., B. B. Balsley, R. F. Woodman, and J. P. McClure, Equatorial Spread *F*: Implications of VHF radar observations, *J. Geophys. Res.*, **75**, 7199–7216, 1970.

Fejer, B. G. and M. C. Kelley, Ionospheric irregularities, *Rev. Geophys. Space Phys.*, **18**, 401–454, 1980.

Fejer, B. G., L. Scheerliess, and E. R. de Paula, Effects of the vertical plasma drift velocity on the generation and evolution of equatorial Spread *F*, *J. Geophys. Res.*, **104**, 19859–19869, 1999.

Fuller-Rowell, T. J., M. V. Codrescu, R. J. Moett, and S. Quegan, On the seasonal response of the thermosphere and ionosphere to geomagnetic storms, *J. Geophys. Res.*, **101**, 2343–2353, 1996.

Haerendel, G., Theory of equatorial Spread *F*, *Report, Max-Plank Inst. Phys. Astrophys.*, Munich, 1973.

Huang, Y. N., K. Cheng, and W. T. Huang, Seasonal and solar cycle variations of Spread *F* at equatorial anomaly crest zone, *J. Geomag. Geoelectr.*, **39**, 639–657, 1987.

Hysell, D. L. and J. Burcham, Long term studies of equatorial spread *F* using the JULIA radar at Jicamarca, *J. Atmos. Terr. Phys.*, **64**, 1531–1543, 2002.

Jyoti, N., C. V. Devasia, R. Sridharan, and D. Tiwari, Threshold height ($h'F_c$) for the meridional wind to play a deterministic role in the bottom side equatorial Spread *F* and its dependence on solar activity, *Geophys. Res. Lett.*, **31**, L12809, doi:10.1029/2004GL019455, 2004.

Kelley, M. C. and J. P. McClure, Equatorial Spread-*F*: a review of recent experimental results, *J. Atmos. Terr. Phys.*, **43**, 427–435, 1981.

Krishna Murthy, B. V., S. S. Hari, and V. V. Somayajulu, Nighttime equatorial thermospheric meridional winds from $h'F$ data, *J. Geophys. Res.*, **95**, 4307–4310, 1990.

Lee, C. C., J. Y. Liu, B. W. Reinisch, W. S. Chen, and F. D. Chiu, The effects of the pre-reversal drift, EIA asymmetry and magnetic activity on ESF during solar minimum, *Ann. Geophys.*, **23**, 745–751, 2005.

Manju, G., C. V. Devasia, and R. Sridharan, On the seasonal varations of the threshold height for the occurrence of equatorial Spread *F* during solar minimum and maximum years, *Ann. Geophys.*, **25**, 1, 2007.

Maruyama, T., A diagnostic model for equatorial Spread *F* 1. Model description and applications to the electric field and neutral wind effects, *J. Geophys. Res.*, **93**, 14611–14622, 1988.

Maruyama, T. and N. Matuura, Longitudinal variability of annual changes in activity of ESF and plasma depletions, *J. Geophys. Res.*, **89**, 10903–109012, 1984.

Sekar, R. and M. C. Kelley, On the combined effects of vertical shear and zonal electric field patterns on nonlinear equatorial Spread *F* evolution, *J. Geophys. Res.*, **103**, 735–755, 1998.

Sekar, R. and R. Raghavarao, Role of vertical winds on the Rayleigh-Taylor instabilities of the nighttime equatorial ionosphere, *J. Atmos. Terr. Phys.*, **49**, 981–985, 1987.

Sridharan, R., D. Pallam Raju, and R. Raghavarao, Precursor to equatorial Spread-*F* in OI 630.0 nm dayglow, *Geophys. Res. Lett.*, **21**, 2797–2800,1994.

Subbarao, K. S. V. and B. V. Krishna Murthy, Seasonal variations of equatorial Spread *F*, *Ann. Geophys*., **12**, 33–39, 1994.

Tsunoda, R. T., Control of the seasonal and longitudinal occurrence of equatorial scintillation by longitudinal gradients in integrated Pedersen conductivity, *J. Geophys. Res*., **90**, 447–456, 1985.

Tulasi Ram, S., P. V. S. Rama Rao, K. Niranjan, D. S. V. V. D. Prasad, R. Sridharan, C. V. Devasia, and Sudha Ravindran, The role of post-sunset vertical drifts in predicting the onset of VHF scintillations during high and low sunspot activity, *Ann. Geophys*., **24**, 1609–1616, 2006.

Whitehead, J., Ionization disturbances caused by gravity waves in the presence of an electrostatic field and background wind, *J. Geophys. Res*., **76**, 238–241, 1971.

Woodman, R. F. and C. LaHoz, Radar observations of *F* region equatorial irregularities, *J. Geophys. Res*., **81**, 5447–5466, 1976.

Zalesak, S. T., S. L. Ossakow, and P. K. Chaturvedi, Nonlinear equatorial Spread *F*: The effects of neutral winds and background Pedersen conductivity, *J. Geophys. Res*., **87**, 151–166, 1982.

G. Manju (e-mail: manju_spl@vssc.gov.in), C. V. Devasia, and S. Ravindran